Electronic Supplementary Material (ESI) for Reaction Chemistry & Engineering.

Combustion Induced Synthesis of Multicomponent Cu-Based Catalysts for autocatalytic CO Hydrogenation to Methanol in Three-Phase Reactor System

Vaibhav Pandey[a], Kamal K. Pant[a*], Sreedevi Upadhyayula[a],

[a]Department of Chemical Engineering, Indian Institute of Technology Delhi, 110016, India

*Corresponding Author: kkpant@chemical.iitd.ac.in

Supplementary Information

Catalyst synthesis:

Catalysts were synthesized by the solvent combustion method using citric acid as organic fuel and adopted from Yao et al [1]. Typically, CuZn, CuMg, and CuZnMg catalysts were prepared from citric acid monohydrate, Copper nitrate trihydrate, zinc nitrate hexahydrate, and magnesium nitrate. The molar ratio of citric acid: (Cu + (Zn or Mg) =2 and the weight ratio of (Cu-Zn-Mg + citric acid)/water =2. The homogeneous aqueous solution was obtained by stirring the initial mixture followed by heating for 2 hours at 50 ºC to obtain a citric acid-based slurry. The slurry was heated overnight at 110 ºC followed by combustion in a muffle furnace at 350 °C for 4 h to produce combusted carbon-free powder. Typically, the molar ratio of Cu: metal oxide is 3:2.

Activity test:

CO hydrogenation reaction was carried out in a stirred tank slurry reactor with 300 ml volume in continuous mode with a typical 5-weight % slurry concentration in diglyme solvent. The typical reactor schematic is shown in Figure S1. The catalyst was reduced in a hydrogen flow of 50 mL/min at 15 bar and 250 ºC for 6 hours at 400 rpm stirring speed. The reactor was cooled to ambient temperature and purged with syngas (CO/H_2= 0.5) and pressurized up to required pressures at a gas flow rate of 100 sccm (WHSV = 2564 $ml\, g_{cat}^{-1} h^{-1}$). The reactor was heated to 220-280 ºC while maintaining the pressure at 30-50 bar using a back pressure regulator. The stirrer speed is maintained at 1000 rpm to eliminate the external mass transfer limitations. The effluent gaseous products were analyzed using a Gas Chromatograph (Agilent technologies 8860 GC) equipped with flame ionization (FID) and thermal conductivity detectors (TCD) in the porapack-Q column and liquid products were analyzed by ALS equipped Gas Chromatograph (Agilent Technologies 7820A GC) equipped with flame ionization detector (FID) and DB-waxtr column.

The syngas conversion and product selectivity were calculated from the following relationships:

$$\%\ CO\ conversion\ (X_{CO}) = \frac{CO_{in} - CO_{out}}{CO_{in}} \times 100\%$$

$$\%\ Selectivity_P = \frac{Total\ moles\ of\ methanol\ formed}{CO_{in} - CO_{out}} \times 100\%$$

$$STY\ (g_{CH_3OH} kg_{cat}^{-1} h^{-1}) = \frac{F_{CO} * X_{CO} * S_{CH_3OH} * M_{CH_3OH}}{22400 * W_{cat}}$$

F_{CO} = Flowrate of CO_{in} (mL/h), X_{CO} = CO Conversion, S_{CH_3OH} = Methanol Selectivity

W_{cat} = Catalyst Weight, M_{CH_3OH} = Molecular weight of methanol

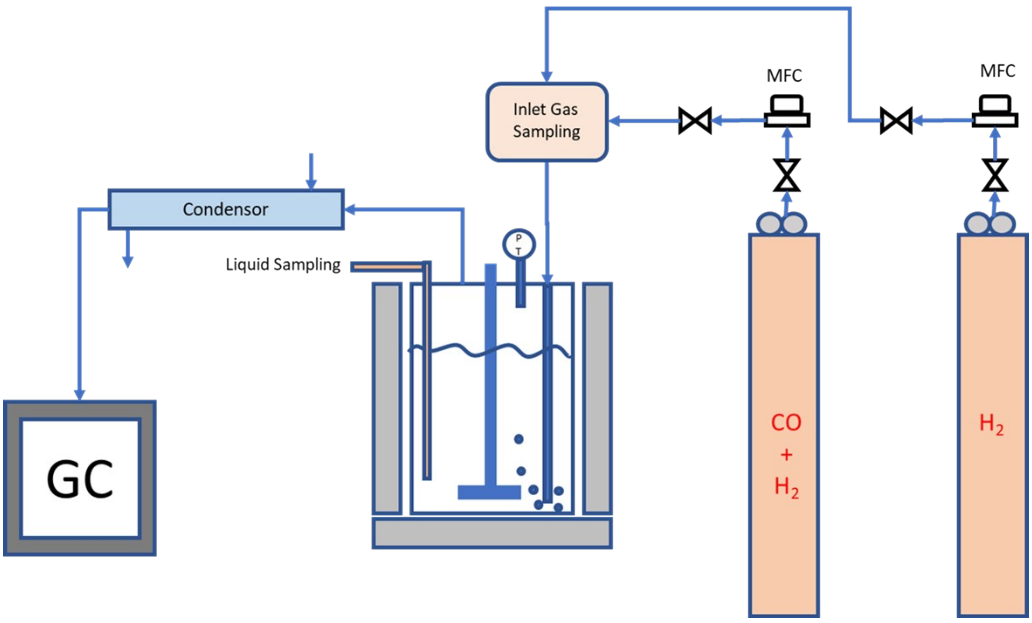

Figure S1: Schematic diagram of stirred tank slurry reactor set-up for methanol synthesis from syngas.

Characterization:

The XRD pattern of catalysts was recorded within the range of 20° to 80° on Rigaku Miniflex 600 using Cu Kα radiation with a scan speed of 4°/min with a step width of 0.02°. The crystallite size was calculated using the Scherrer equation.

The surface area was determined by N_2 physisorption at 77K using Quantachrome Autosorb (IQ-C-XR-AG) surface area analyzer. The sample was degassed at 473K for 2 hours before analysis. The surface area and pore size distribution were analyzed by Brunauer-Emmett-Teller (BET) method and Non-linear Density Function Theory (NLDFT) method, respectively.

H_2-TPR experiments were carried out in Quantachrome Autosorb (IQ-C-XR-AG) instrument. The calcined catalysts (~40mg) were outgassed for 2 h at 200 °C in argon flow (30mL/min). The H_2- TPR was carried out from 100 °C to 800 °C at the ramp rate of 10 °C/min with an H_2 (10.2 vol% H_2) flow of 30 mL/min and a TCD detector was used to calculate the hydrogen consumption and plotted against temperature.

The CO_2 TPD and H_2-TPD were performed in the Quantachrome Autosorb (IQ-C-XR-AG) instrument and followed the same procedure of pre-treatment. The calcined catalysts (~100mg) were reduced *in-situ* at 400 °C for 2 h in the flow of 10.2% H_2 followed by 5.1% CO_2 and 10.2% H_2 adsorption at 80 °C for 60 min. After He purges for 30 min, the desorption profile of H_2 and CO_2 was recorded from 40°C to 850°C at 10°C/min with the TCD.

The surface morphology of combusted catalysts was analyzed by the FESEM instrument of JEOL (7800F Prime). HR-TEM images of the combusted catalysts were acquired by using an FEI TecnaiTF20 microscope. The surface chemical states of the catalysts were studied by X-ray photoelectron spectroscopy (XPS) on PHI 5000 Versa Probe III with an Al Kα.

The copper (Cu^0) surface area (S_c) and dispersion was analyzed by the nitrous oxide (N_2O) pulse method. The catalysts were first reduced at 400 °C for 2h with 10.2%H_2 followed by purging with He for 1 h and cooled down to 40 °C. The catalysts were then exposed to 10% N_2O for 2 h to oxidize surface Cu atoms to Cu_2O. After cooling to room temperature, the temperature-programmed reduction (TPR) was performed with 10.2% H_2 flow to reduce the Cu_2O to Cu^0 at 10 °C /min ramp rate to 700 °C. The dispersion, Cu surface area, and particle size were calculated from the amount of H_2 consumed during the TPR step by assuming that Cu crystallites are spherical in nature. The dispersion of Cu, copper surface area (S_c), and particle size were calculated from the following equations (SE6, SE7, and SE8).

Computational Details:

All computations were done in Dessault Systems' Materials Studio using the Dmol^3 program package. DFT [2] was used with Perdew-Wang-91 (PW-91) [27] and generalized gradient approximation (GGA) exchange-correlation function with unrestricted spin polarization. PW-91 functional is reliable for this calculation system, according to previous reports [45]. Double numerical basis with polarization (DNP) was used for all atoms in the adsorbed and substrate system [6]. Effective core potentials (ECP) are used for ZnO and MgO atoms [7]. The converge criterion judged by energy, force, and displacement are 1×10^{-5} Ha, 0.002 Ha/Å, and 0.005 Å respectively. The Monkhorst–Pack grid of 4×4×1 [8] and Methfessel–Paxton smearing of 0.01 Hartree (Ha) were used in the k-point sampling approach. The electronic structures were obtained by solving the Kohn-Sham equation [910].

The estimated lattice constant of bulk ZnO and MgO was 3.249 Å and 4.211 Å which is in the agreement with the experimental value of 3.25 Å [11] and 4.19 Å [12] respectively. A good agreement was found between our computed data and experimental data. MgO (200) and ZnO (101) facet was cleaved from the optimization bulk using 5 layered p(2×2) supercell and vacuum region of 20 Å was used to model 0.20 monolayer (ML) coverage. In optimized 5 layered supercell the top three layers were relaxed, whereas the bottom two layers were fixed, and the volume remained constant.

Adsorption energy was calculated in vacuum by:

$$\Delta E_{ads} = E_{surface/adsorbent} - (E_{surface} + E_{adsorbent}) \quad \text{(SE1)}$$

Calculation of the dimensionless number (Su)

The dimensionless suspension number to assess the degree of the catalyst dispersion in the solvent was calculated as follows [13]

$$Su = \frac{\rho_{liq}.n^3.d_R^5}{\varphi_v.(\rho_{cat} - \rho_{liq}).g.w_{ss}} \quad \text{(SE2)}$$

Where ρ_{cat} and ρ_{liq} are the density of the solvent and catalyst, respectively, n is the stirrer speed, dR is the diameter of the stirrer bar, φ_v is the vol/vol of catalyst and suspension, g is the acceleration of the gravity and w_{ss} is the sedimentation of swarm particles.

the sedimentation of swarm particles

$$w_{ss} = \sqrt{\frac{4}{3} \cdot \left(\frac{\rho_{cat}}{\rho_{liq}} - 1\right) . \frac{g \cdot d_{cat}}{C_D}} \quad \text{(SE3)}$$

the drag coefficient CD is a function of Reynolds number (Re)

$$Re = \frac{w_{ss} \cdot \rho_{liq} \cdot d_{cat}}{\eta_{liq}} \quad \text{(SE4)}$$

$$CD = \frac{24}{Re} + \frac{4}{Re^{0.5}} + 0.4 \quad \text{(Valid for } 0 < Re < 1.5 \times 10^{-5}\text{)} \quad \text{(SE5)}$$

Table S1: the suspension number and stirrer speed of the catalysts

	Suspension Number (Su)		
Catalysts	300 rpm ($\times 10^{-5}$)	1000 rpm ($\times 10^{-5}$)	1500 rpm ($\times 10^{-5}$)
CuZn	1.328	49.21	166
CuMg	5.724	212	715.5
CuZnMg	2.932	108.6	366.5

Calculation of the Cu dispersion, Cu^0 surface area, and particle size

The dispersion of Cu and copper surface area (S_c) was calculated from the equations (SE6) and (SE7):

$$D = \frac{\left(\frac{2n_{H_2} \times M_{Cu}}{W}\right) \times 100\%}{X} \times 100\% \tag{SE6}$$

$$S_{Cu} = \frac{2n_{H_2} \times N}{1.4 \times 10^{19} \times W} (m^2 g^{-1}) \tag{SE7}$$

where n_{H_2} is the molar number of consumed H_2, D is the dispersion of Cu, M_{Cu} is the relative atomic mass (63.546 g mol^{-1}), W is the weight of the catalyst, and X is the stoichiometric composition of Cu (wt.%); S_{Cu} is the exposed copper surface area per gram catalyst, N is Avogadro's constant (6.02 $\times 10^{23}$ atoms mol^{-1}), and 1.4×10^{19} is the number of copper atoms per square meter.

The mean Cu particle size is defined, by the following equation when the particles are hemispherical in shape.

$$d_p = \frac{6 * M}{D * \rho_{Cu} * \sigma * N_A} \tag{SE8}$$

Where M is the molecular weight of Cu (63.546 g mol^{-1})
D is the Cu fractional dispersion obtained as explained above
ρ is the Cu metal density (8.94 g cm^{-3}),
σ is the area occupied by a surface Cu atom (6.85 $Å^2$ per atom),
and NA is the Avogadro constant

The d-band center is calculated by:

$$\varepsilon_d = \int_{-\infty}^{\infty} E\rho_d(E)d\varepsilon / \int_{-\infty}^{\infty} \rho_d(E)d\varepsilon \tag{SE9}$$

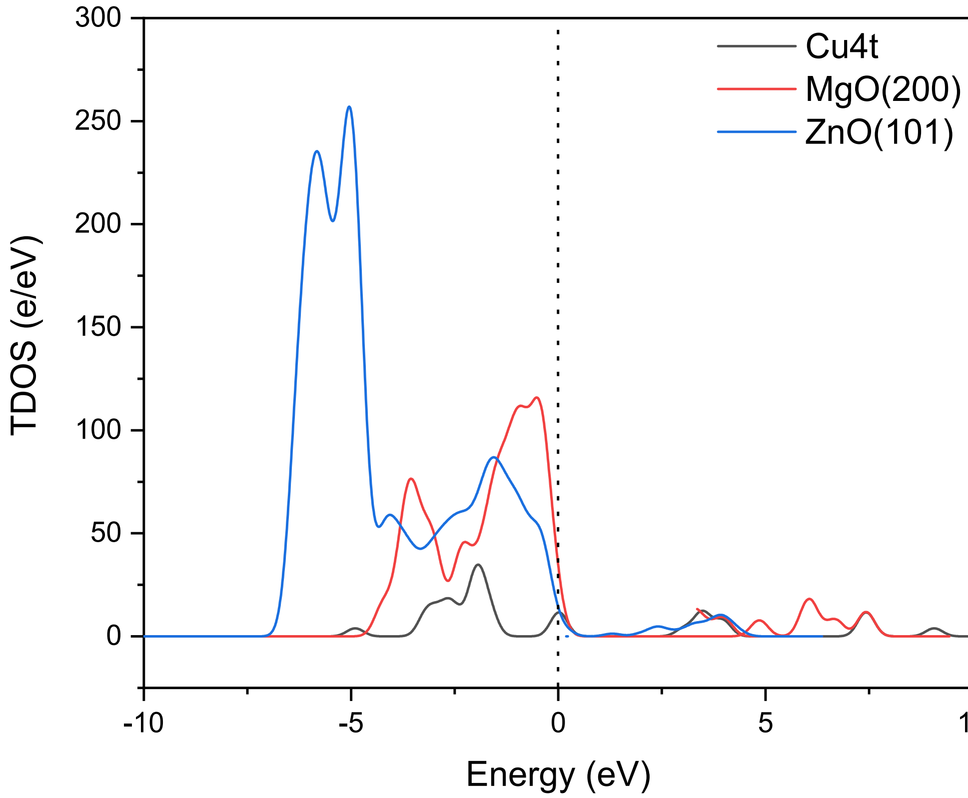

Figure S2: Total density of states (TDOS) of Cu_{4t}, MgO(200), and ZnO(101). The Fermi level is set to zero.

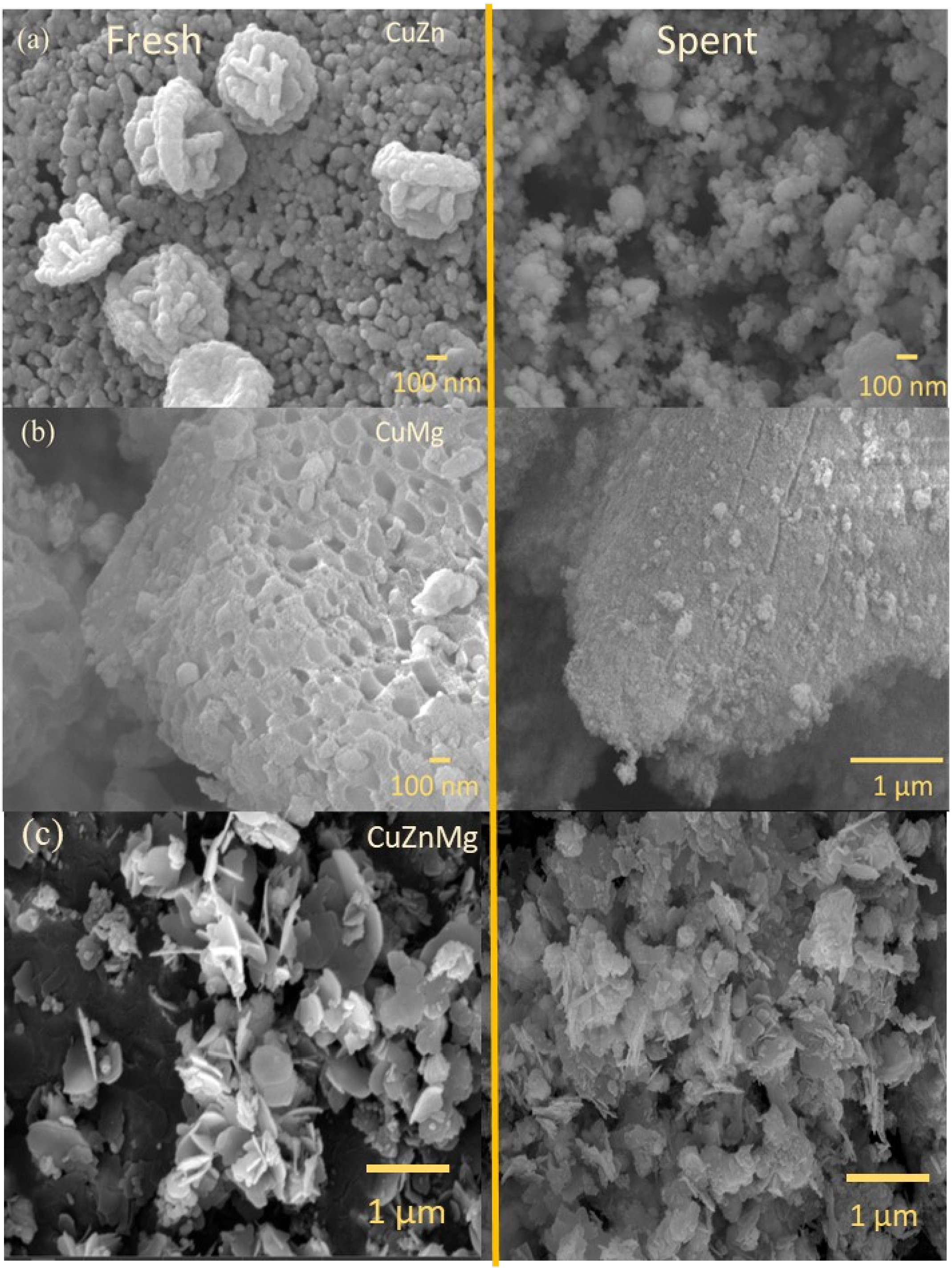

Figure S3: SEM images of the fresh and spent catalyst (a) CuZn, (b) CuMg, (c) CuZnMg

References

1 B. Yao, T. Xiao, O. A. Makgae, X. Jie, S. Gonzalez-Cortes, S. Guan, A. I. Kirkland, J. R. Dilworth, H. A. Al-Megren, S. M. Alshihri, P. J. Dobson, G. P. Owen, J. M. Thomas and P. P. Edwards, *Nat. Commun.*,2020,11, 6395

2 B. Delley, *J. Chem. Phys.*, 1990, **92**, 508–517.

3 J. P. Perdew and Y. Wang, *Phys. Rev. B*, 1992, **45**, 13244–13249.

4 Z. Jiang and T. Fang, *Appl. Surf. Sci.*, 2016, **376**, 219–226.

5 W. H. Jiao, S. Z. Liu, Z. J. Zuo, R. P. Ren, Z. H. Gao and W. Huang, *Appl. Surf. Sci.*, 2016, **387**, 58–65.

6 Y. Inada and H. Orita, *J. Comput. Chem.*, 2008, **29**, 225–232.

7 R. Zhang, L. Ling, B. Wang and W. Huang, *Appl. Surf. Sci.*, 2010, **256**, 6717–6722.

8 Z. Zuo, L. L. Sun, W. Huang, P. Han and Z. Li, *Appl. Catal. A Gen.*, 2010, **375**, 181–187.

9 M. Dolg, W. Liu and S. Kalvoda, *Int. J. Quantum Chem.*, 2000, **76**, 359–370.

10 Hohenberg, P.; Kohn, W. Phys. Rev. 1964, 136, B864−B871

11 H. Algarni, A. Gueddim, N. Bouarissa, M. A. Khan and H. Ziani, *Results Phys.*, 2019, **15**, 102694.

12 M. I. McCarthy and N. M. Harrison, *Phys. Rev. B*, 1994, **49**, 8574–8582.

13 P. Schühle, S. Reichenberger, G. Marzun and J. Albert, *Chemie-*

Ingenieur-Technik, 2021, **93**, 585–593.